Kinetic and Thermodynamic Studies of Ce(IV)-Mediated Oxidation of β-Dicarbonyls: Solvent-Dependent Behavior of Radical Cation Intermediates

*Jingliang Jiao, Yang Zhang, Luna Xu, Jennifer Deng, and Robert A. Flowers II**

Department of Chemistry, Lehigh University, Bethlehem, PA 18015

Supporting Information

List of Contents **page number**

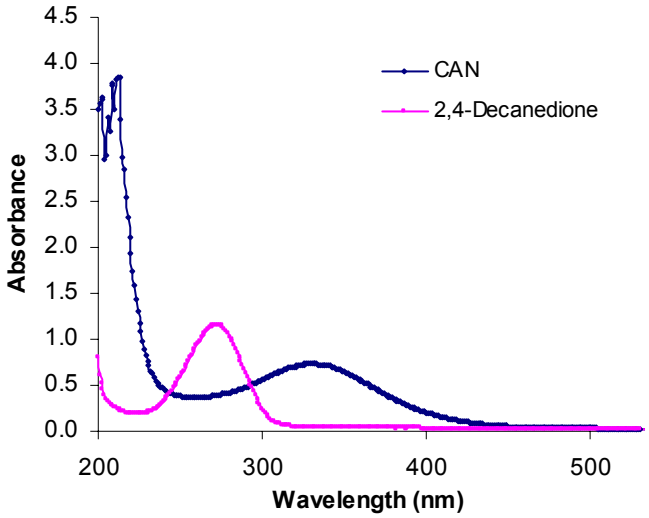

Figure S1. UV-vis spectrum of CAN and 2,4-decanedione in CH_3CN, [CAN]=0.1 mM, [diketone]=0.1 mM

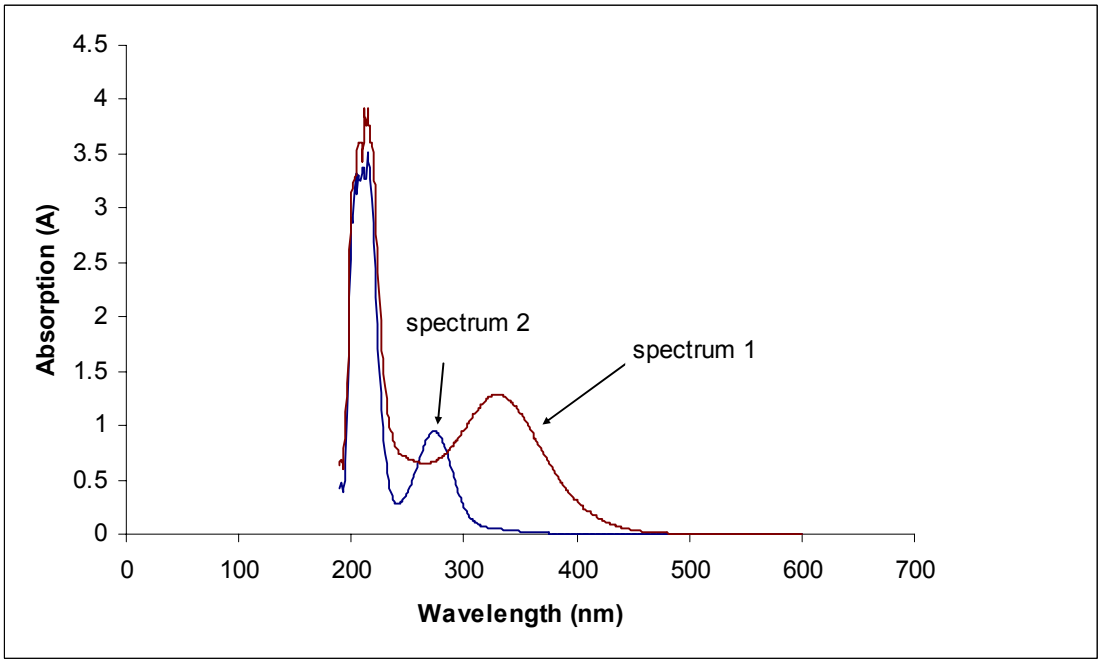

Figure S2 Comparison of UV-visible spectra of CAN before and after reaction with 2,4-pentanedione. Spectrum 1 represents CAN in CH_3CN. Spectrum 2 represents the UV-visible spectrum of the Ce(III) salt formed after reaction with 2,4 pentanedione.

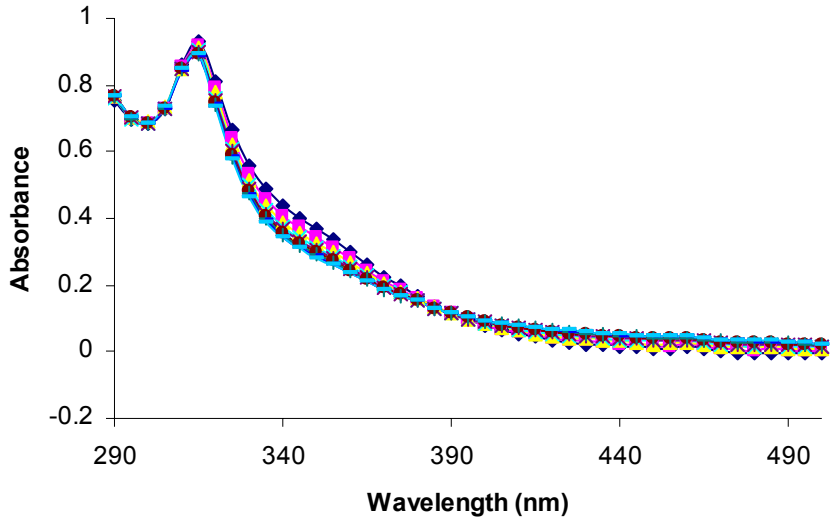

Figure S3. Time-resolved absorption spectrum observed from CAN and 2,4-decanedione in CH_3CN in the range of 290-500 nm ([diketone]:[CAN]=20 mM:1 mM) at 25 ^oC

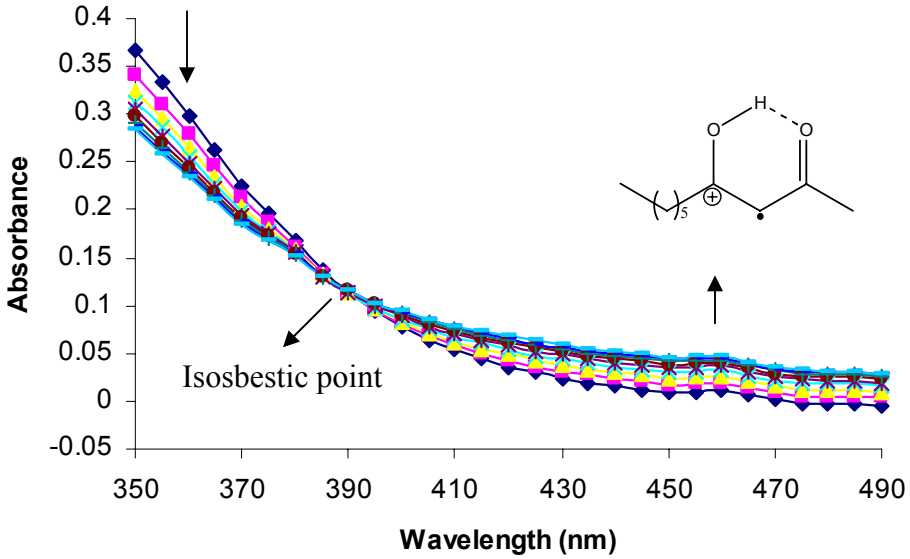

Figure S4. Time-resolved absorption spectrum observed from CAN and 2,4-decanedione in CH_3CN in the range of 360-500 nm ([diketone]:[CAN]=20 mM:1 mM) at 25 ^oC

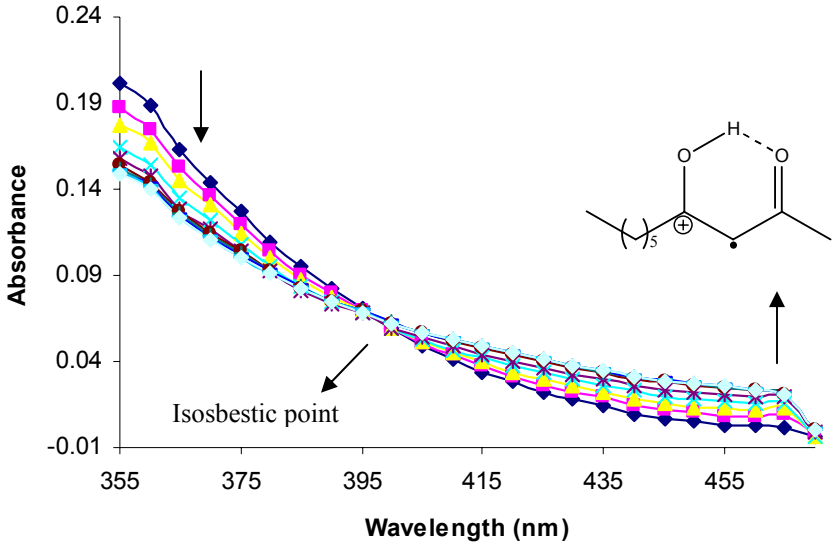

Figure S5. Time-resolved absorption spectrum observed from CTAN and 2,4-decanedione in CH_2Cl_2 in the range of 355-470 nm ([diketone]:[CTAN]=20 mM:1 mM) at 25 ^oC

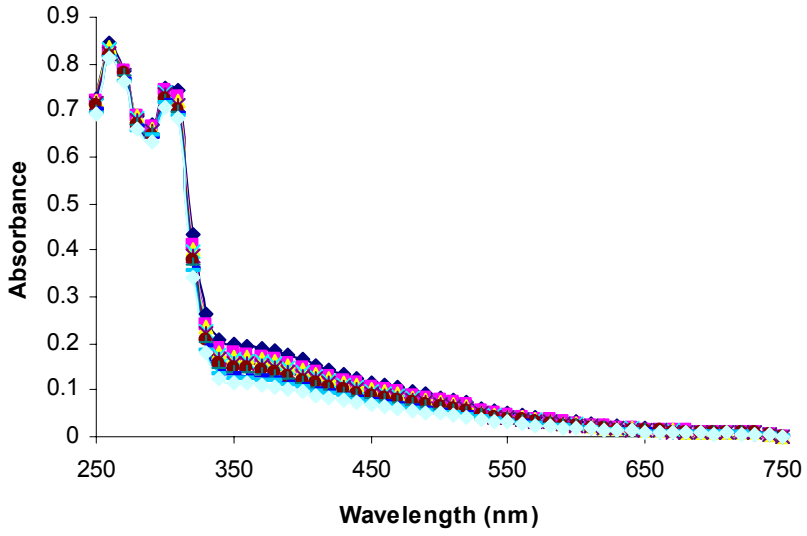

Figure S6. Time-resolved absorption spectrum observed from CAN and 2,4-decanedione in CH_3OH in the range of 250-750 nm ([diketone]:[CAN]=20 mM:1 mM) at 25 ^oC

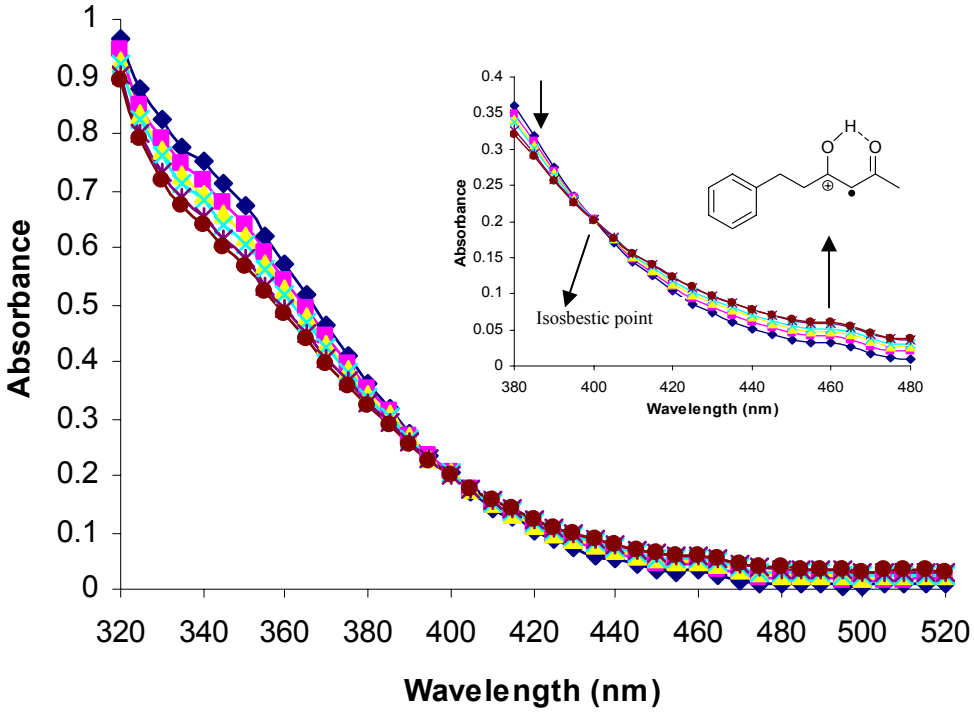

Figure S7. Time-resolved absorption spectrum observed from CTAN and 6-phenyl-2,4-hexanedione in CH_2Cl_2 in the range of 320-520 nm ([diketone]:[CTAN]=20 mM:1 mM) at 25 ^oC. Inset: Wavelength range of 380-480 nm

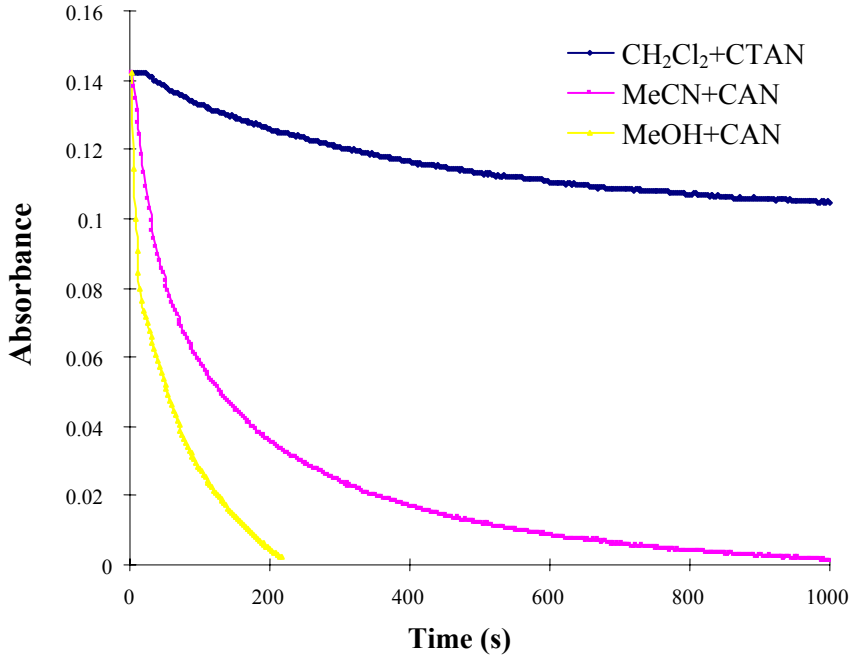

Figure S8. Typical stopped-flow trace for the decay of radical cation at 460 nm generated from Ce(IV) reagents and 2,4-pentanedione in different solvents at 25 ^oC

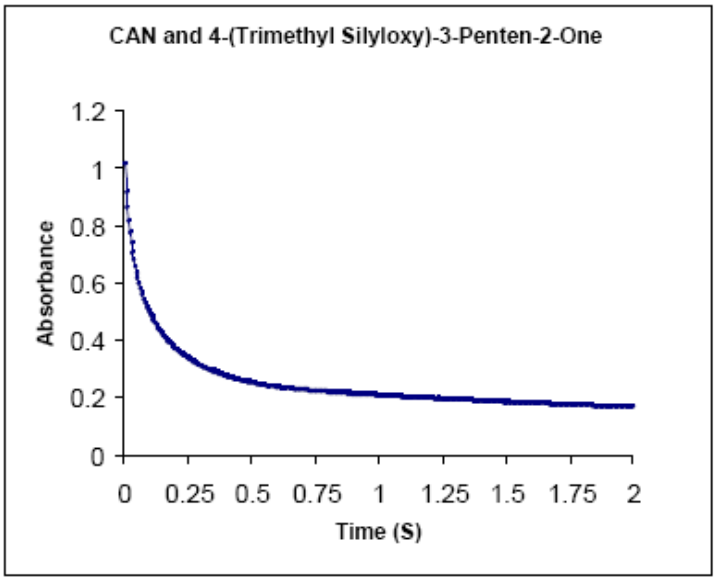

Figure S9. Stopped-flow trace showing the decay of CAN at 330 nm in the presence of 4-(trimethyl silyloxy)-3-penten-2-one in CH_3CN at 25 ^oC

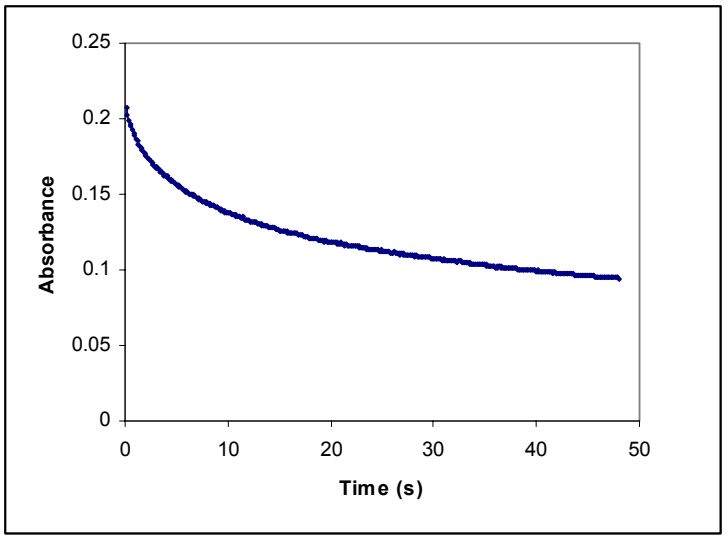

Figure S10. Stopped-flow trace showing the decay of CTAN at 330 nm in the presence of 4-(trimethyl silyloxy)-3-penten-2-one in CH_2Cl_2 at 25 ^oC

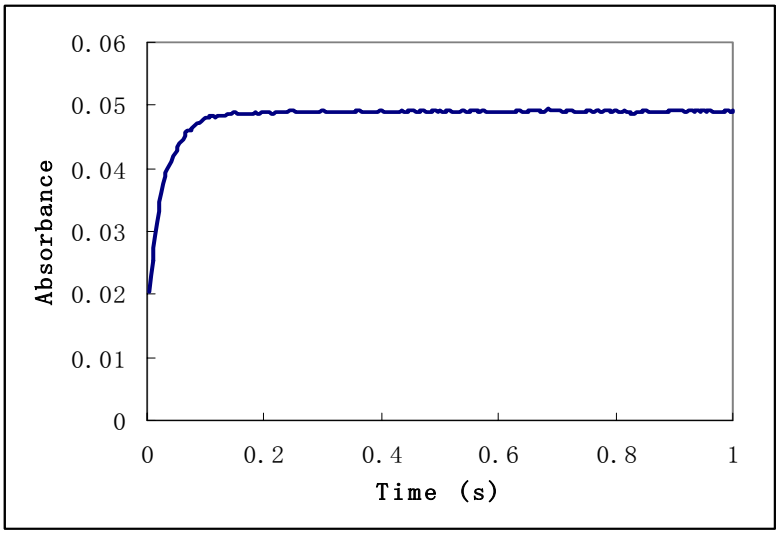

Figure S11. Stopped-flow trace showing radical cation formation at 460 nm generated from CTAN and 4-(trimethyl silyloxy)-3-penten-2-one in CH_2Cl_2 at 25 ^oC

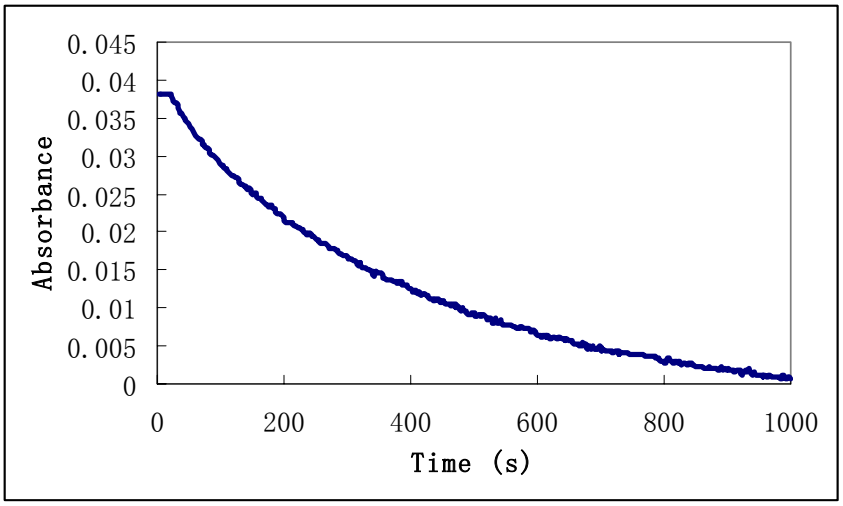

Figure S12. Stopped-flow trace showing radical cation decay at 460 nm generated from CTAN and 4-(trimethyl silyloxy)-3-penten-2-one in CH_2Cl_2 at 25 ^oC

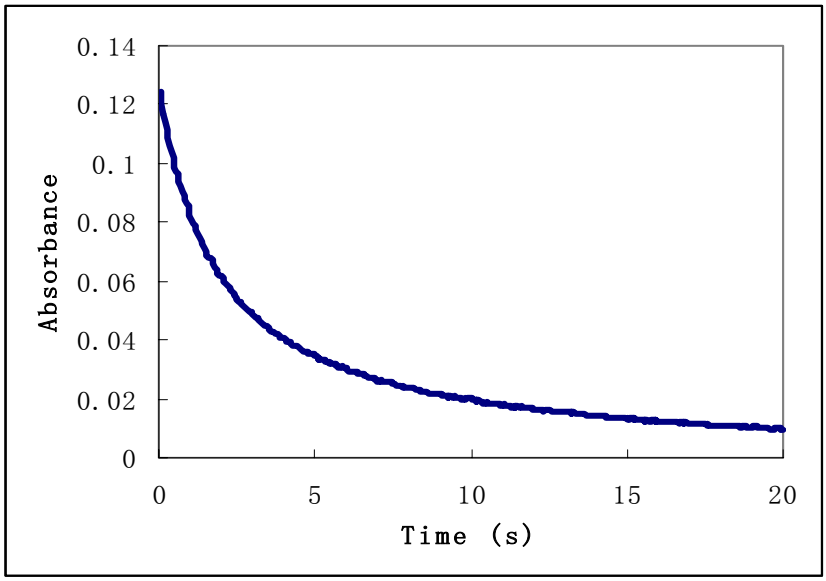

Figure S13. Stopped-flow trace showing the decay of CAN at 330 nm in the presence of 4-(trimethyl silyloxy)-3-penten-2-one in CH_3OH at 25 ^oC

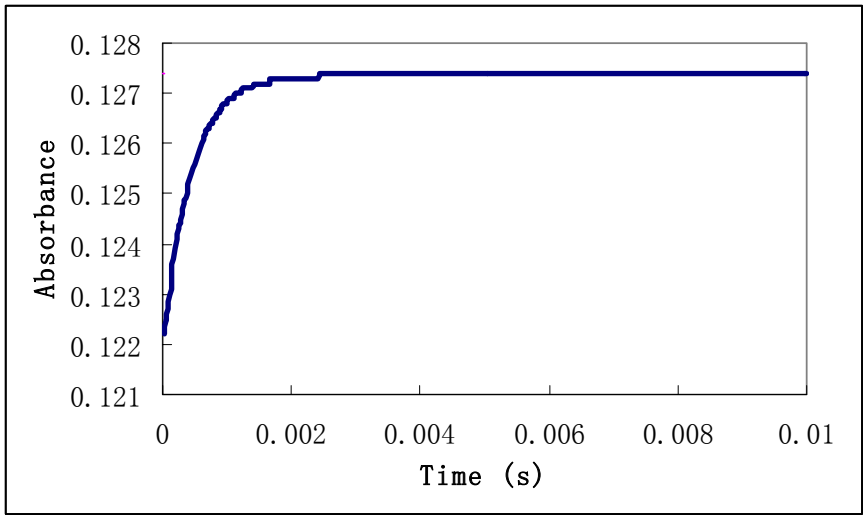

Figure S14. Stopped-flow trace showing radical cation formation at 460 nm generated from CAN and 4-(trimethyl silyloxy)-3-penten-2-one in CH_3OH at 25 ^oC

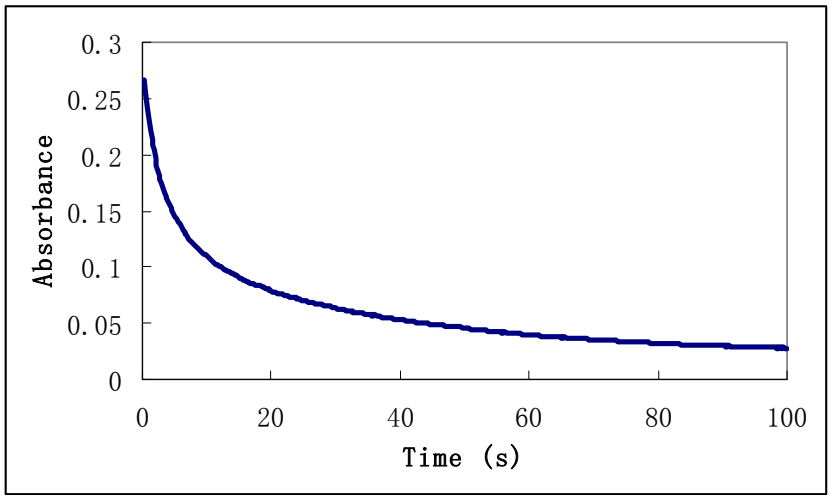

Figure S15. Stopped-flow trace showing radical cation decay at 460 nm generated from CAN and 4-(trimethyl silyloxy)-3-penten-2-one in CH_3OH at 25 ^oC

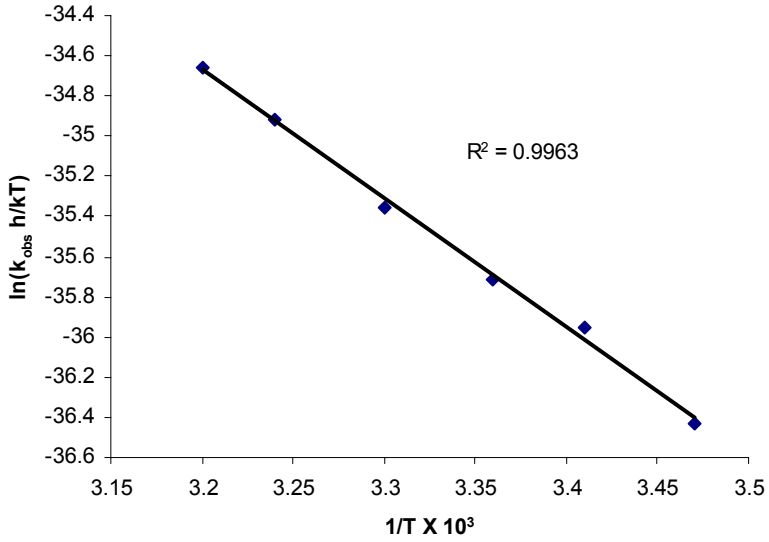

Figure S16. Eyring plot for CTAN and 6-phenyl-2,4-hexanedione in CH_2Cl_2

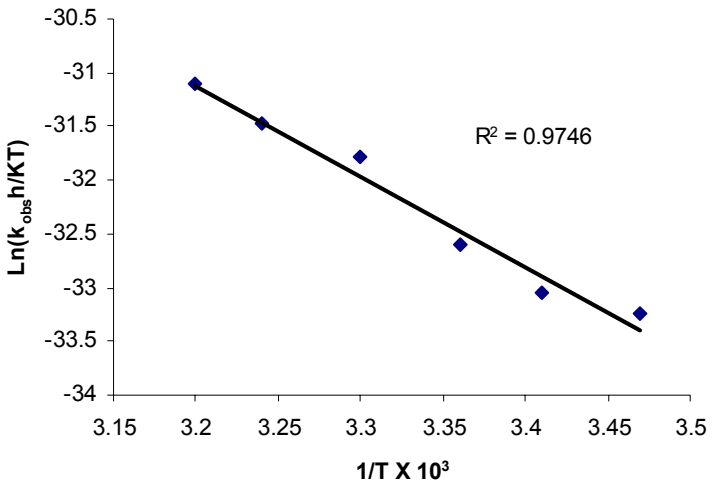

Figure S17. Eyring plot for CAN and 6-phenyl-2,4-hexanedione in CH_3CN

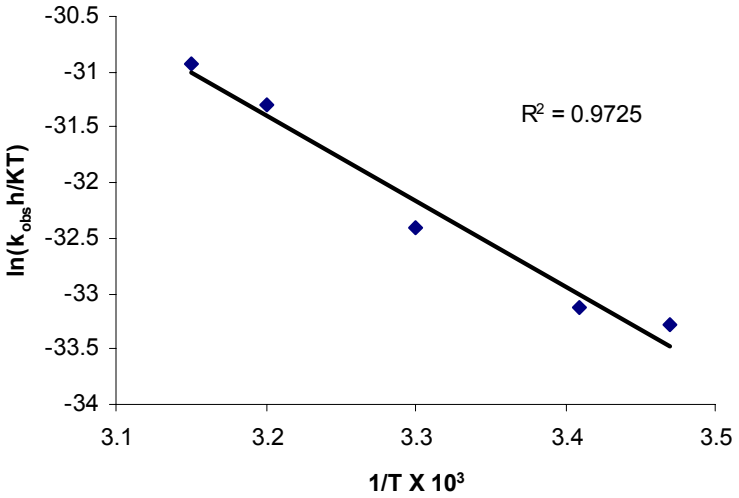

Figure S18. Eyring plot for CTAN and 6-phenyl-2,4-hexanedione in CH_3CN

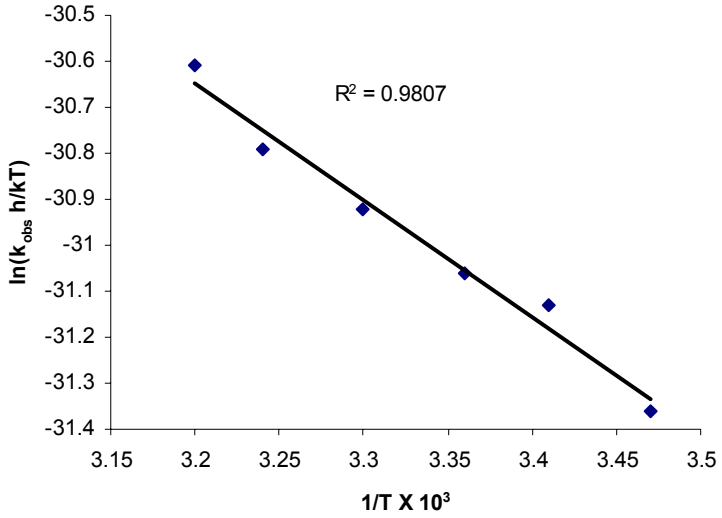

Figure S19. Eyring plot for CAN and 6-phenyl-2,4-hexanedione in CH_3OH

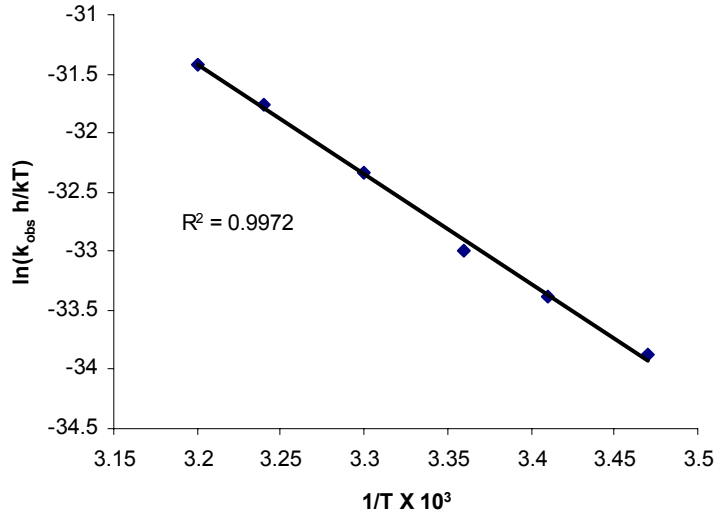

Figure S20. Eyring plot for CAN and 2,4-petanedione in CH_3CN

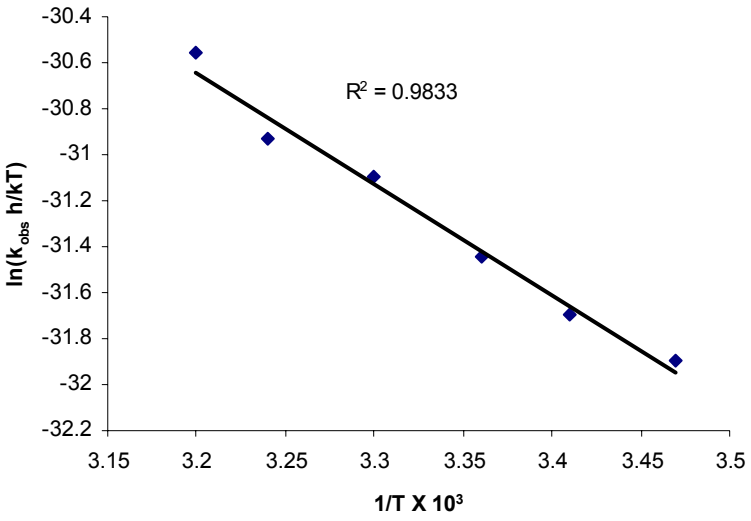

Figure S21. Eyring plot for CAN and 2,4-petanedione in CH_3OH

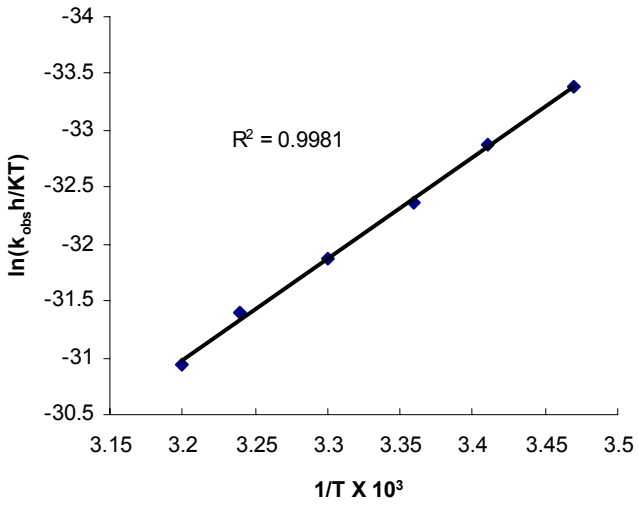

Figure S22. Eyring plot for CTAN and 2,4-petanedione in CH_3CN

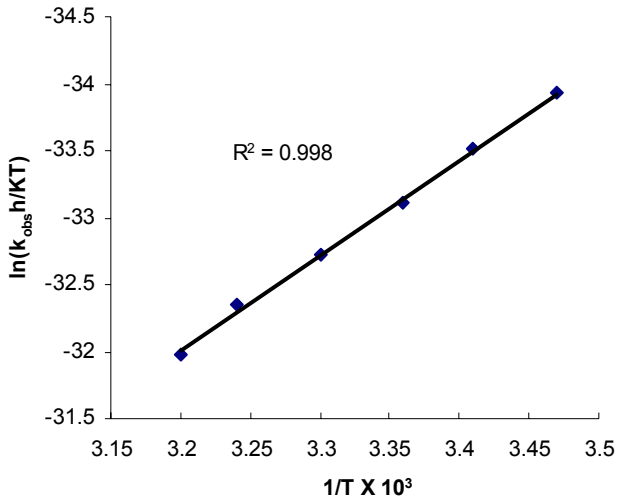

Figure S23. Eyring plot for CTAN and 2,4-petanedione in CH_2Cl_2

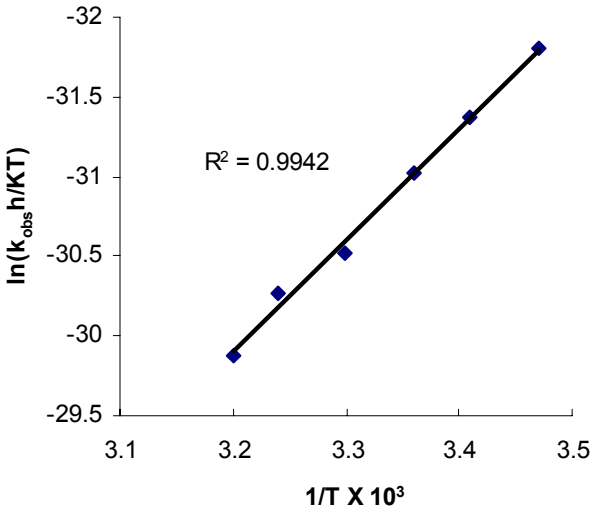

Figure S24. Eyring plot for CAN and 4-(trimethyl silyloxy)-3-penten-2-one in CH_3OH

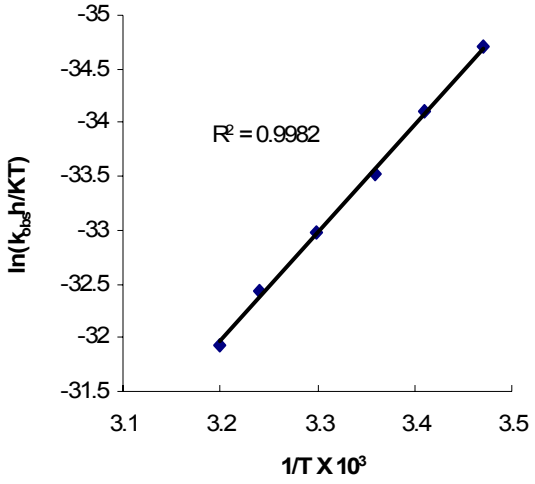

Figure S25. Eyring plot for CAN and 4-(trimethyl silyloxy)-3-penten-2-one in CH_3CN

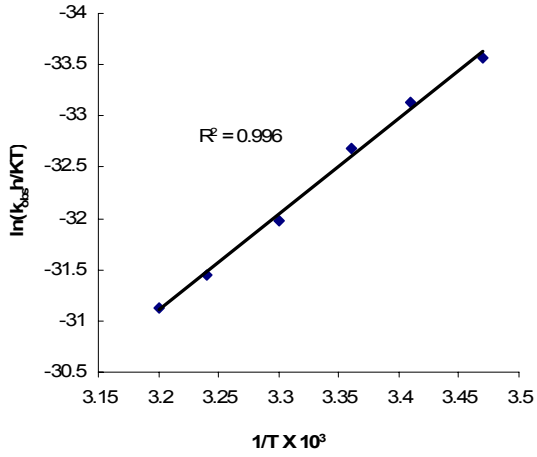

Figure S26. Eyring plot for CTAN and 4-(trimethyl silyloxy)-3-penten-2-one in CH_3CN

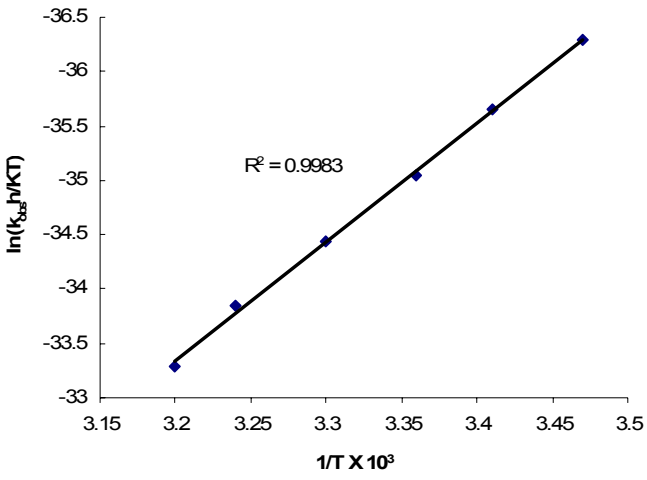

Figure S27. Eyring plot for CTAN and 4-(trimethyl silyloxy)-3-penten-2-one in CH_2Cl_2

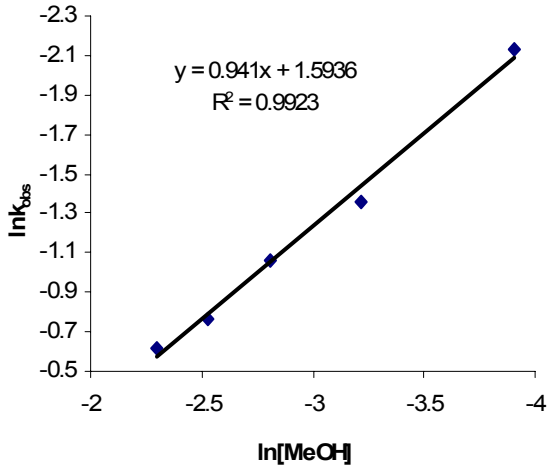

Figure S28. Plot for determination of reaction order of CH_3OH in the decay of $\mathbf{4}^{+\cdot}$ in CH_2Cl_2

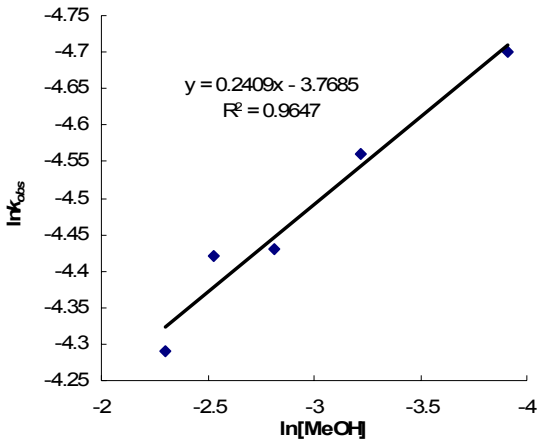

Figure S29. Plot for determination of reaction order of CH_3OH in the decay of $\mathbf{4}^{+\cdot}$ in CH_2Cl_2.

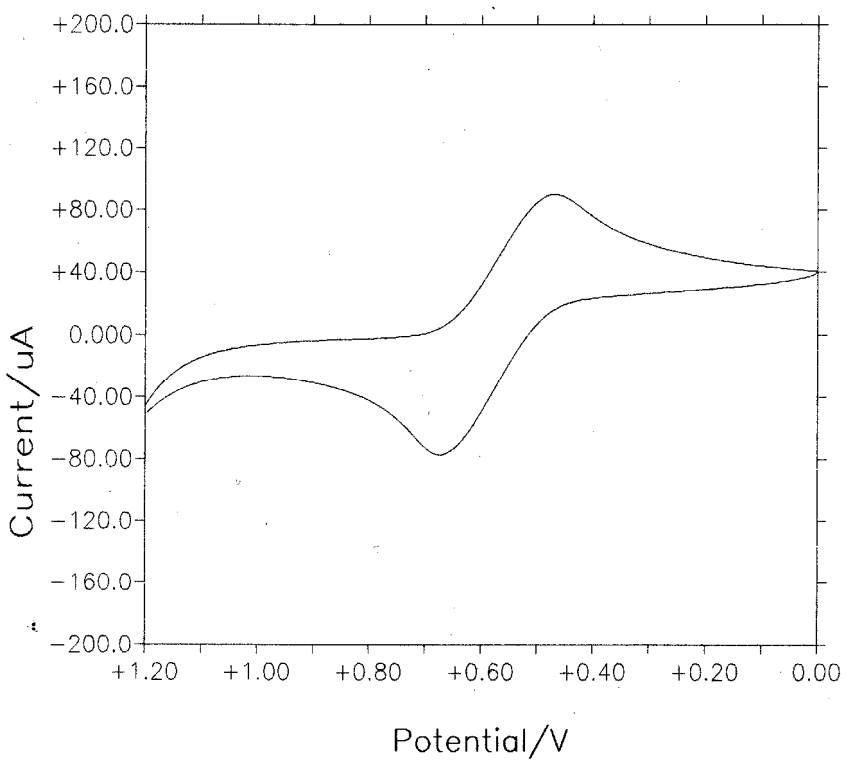

Figure S30. Cyclic Voltammogram of CAN in MeOH. $E_{1/2}$ = 570 ± 20 mV vs. sat'd $Ag/AgNO_3$ reference electrode.

The redox potentials of CAN in MeOH was measured by cyclic voltammetry with a BAS 100B electrochemical analyzer. The working electrode was a standard glassy carbon electrode. The auxiliary electrode was a platinum wire and a saturated $Ag/AgNO_3$ electrode was used as the reference electrode. The electrolyte was tetrabutylammonium hexafluorophosphate. All measurements were repeated twice and no significant experimental error was observed between the two measurements.

The experimental conditions were as follows:

Initial E (mV) = 1200	Sweep rate (mV/s) = 100
Final E (mV) = 0	Quiet T (s) = 2
	Sensitivity = (A/V) =1 x 10-5

Synthesis and NMR data for compounds 1, 1-Acetyl-2-tetralone, and 6

6-Phenyl-2,4-hexanedione (1)[1]

6-Phenyl-2,4-hexanedione was prepared as a keto-enol mixture in 82% yield by the reaction of 2,4-pentanedione and (2-bromo-ethyl)-benzene following the reported procedure.[1] ^{1}H NMR (500MHz, $CDCl_3$): (enol isomer) δ 15.43 (s, 1H); 7.28 (m, 2H); 7.14 (m, 3H); 5.46 (s, 1H); 2.91 (t, J = 7.1 Hz, 2H); 2.57 (t, J = 7.1 Hz, 2H); 2.02 (s, 3H). ^{13}C NMR (125MHz, $CDCl_3$): δ 193.3, 191.1, 137.6, 135.7, 129.2, 128.1, 100.0, 40.1, 31.1, 24.8.

1-Acetyl-2-tetralone[2]

1-Acetyl-2-tetralone was obtained in 73% yield following the representative procedure described in the experimental section. ^{1}H NMR (500MHz, $CDCl_3$): (enol isomer) δ 16.51 (s, 1H); 7.52-7.00 (m, 4H); 2.84 (t, J = 7.0 Hz, 2H); 2.54 (t, J = 7.0 Hz, 2H); 2.36 (s, 3H). ^{13}C NMR (125MHz, $CDCl_3$): δ 200.0, 183.8, 128.8, 128.5, 127.4, 126.5, 126.2, 125.5, 115.2, 35.3, 27.8, 23.3.

3-(Trimethylsilyloxy)cyclohex-2-en-1-one (6)[3]

Compound **7** was synthesized in 68% yield following the reported procedure.[3] ^{1}H NMR (500MHz, $CDCl_3$): δ 5.37 (t, J = 0.7 Hz, 1H); 2.36 (td, J = 6.2, 0.7 Hz, 2H); 2.32 (t, J = 6.7 Hz, 2H); 1.97 (m, 2H); 0.30 (s, 9H). ^{13}C NMR (125MHz, $CDCl_3$): δ 197.2, 172.5, 106.4, 38.3, 30.8, 23.6, 2.2.

References:

1. Huckin, S. N.; Weiler, L. *J. Am. Chem. Soc.* **1974**, *96*, 1082-1087.
2. Beam, C. F.; Bissell, R. L.; Hauser, C. R. *J. Org. Chem.* **1970**, *35*, 2083-2085.
3. Olah, G. A.; Gupta, B. G. B.; Narang, S. C.; Malhotra, R. *J. Org. Chem.* **1979**, *44*, 4272-4275.